



SNOW DEPTH AND SNOW EXTENT
USING VHRR DATA FROM THE NOAA-2 SATELLITE

David F. McGinnis, Jr.
John A. Pritchard
Donald R. Wiesnet

Washington, D.C.
February 1975

POLAR
PAM
1837

POLARPAM

aa

NATIONAL OCEANIC AND
ATMOSPHERIC ADMINISTRATION

National Environmental
Satellite Service

Pam: 551.321.7 MGT

NOAA TECHNICAL MEMORANDUMS

National Environmental Satellite Service Series

The National Environmental Satellite Service (NESS) is responsible for the establishment and operation of the environmental satellite systems of NOAA.

NOAA Technical Memorandums facilitate rapid distribution of material that may be preliminary in nature and so may be published formally elsewhere at a later date. Publications 1 through 20 and 22 through 25 are in the earlier ESSA National Environmental Satellite Center Technical Memorandum (NESCTM) series (listed in NESS 30). The current NOAA Technical Memorandum NESS series includes 21, 26, and subsequent issuances.

Publications listed below are available from the National Technical Information Service, U.S. Department of Commerce, Sills Bldg., 5285 Port Royal Road, Springfield, Va. 22151. Prices on request. Order by accession number (given in parentheses). Information on memorandums not listed below can be obtained from Environmental Data Service (D831), 3300 Whitehaven St., NW, Washington, D.C. 20235.

NOAA Technical Memorandums

- NESS 21 Geostationary Satellite Position and Attitude Determination Using Picture Landmarks. William J. Dambeck, August 1972, 20 pp. (COM-72-10916)
- NESS 26 Potential of Satellite Microwave Sensing for Hydrology and Oceanography Measurements. John C. Alishouse, Donald R. Baker, E. Paul McClain, and Harold W. Yates, March 1971, 16 pp. (COM-71-00544)
- NESS 27 A Review of Passive Microwave Remote Sensing. James J. Whalen, March 1971, 8 pp. (COM-72-10546)
- NESS 28 Calculation of Clear-Column Radiances Using Airborne Infrared Temperature Profile Radiometer Measurements Over Partly Cloudy Areas. William L. Smith, March 1971, 12 pp. (COM-71-00556)
- NESS 29 The Operational Processing of Solar Proton Monitor and Flat Plate Radiometer Data. Henry L. Phillips and Louis Rubin, May 1972, 20 pp. (COM-72-10719)
- NESS 30 Limits on the Accuracy of Infrared Radiation Measurements of Sea-Surface Temperature From a Satellite. Charles Braun, December 1971, 28 pp. (COM-72-10898)
- NESS 31 Publications and Final Reports on Contracts and Grants, 1970. NESS, December 1971, 6 pp. (COM-72-10303)
- NESS 32 On Reference Levels for Determining Height Profiles From Satellite-Measured Temperature Profiles. Christopher M. Hayden, December 1971, 15 pp. (COM-72-50393)
- NESS 33 Use of Satellite Data in East Coast Snowstorm Forecasting. Frances C. Parmenter, February 1972, 21 pp. (COM-72-10482)
- NESS 34 Chromium Dioxide Recording--Its Characteristics and Potential for Telemetry. Florence Nesh, March 1972, 10 pp. (COM-72-10644)
- NESS 35 Modified Version of the Improved TIROS Operational Satellite (ITOS D-G). A. Schwalb, April 1972, 48 pp. (COM-72-10547)
- NESS 36 A Technique for the Analysis and Forecasting of Tropical Cyclone Intensities From Satellite Pictures. Vernon F. Dvorak, June 1972, 15 pp. (COM-72-10840)
- NESS 37 Some Preliminary Results of 1971 Aircraft Microwave Measurements of Ice in the Beaufort Sea. Richard J. DeRycke and Alan E. Strong, June 1972, 8 pp. (COM-72-10847)
- NESS 38 Publications and Final Reports on Contracts and Grants, 1971. NESS, June 1972, 7 pp. (COM-72-11115)
- NESS 39 Operational Procedures for Estimating Wind Vectors From Geostationary Satellite Data. Michael T. Young, Russell C. Doolittle, and Lee M. Mace, July 1972, 19 pp. (COM-72-10910)
- NESS 40 Convective Clouds as Tracers of Air Motion. Lester F. Hubert and Andrew Timchalk, August 1972, 12 pp. (COM-72-11421)

(Continued on inside back cover)

ERRATA for NOAA Technical Memorandum NESS 63

"Snow Depth and Snow Extent using VHRR Data from the NOAA-2 Satellite"

Page 1, Abstract, line 16: 211 should be 201.

Page 2, Figure 1, caption: Feb. 1-10 should be Feb. 9-10.

Page 3, Figure 2, caption: (0.5-0.6 μ m) should be (0.6-0.7 μ m)

Page 3, paragraph beginning "Most important of the sensors...": Insert
on line 3 following "(0.6-0.7 μ m)" the following: "and thermal
(10.5-12.5 μ m)"

Rec'd: MAR 5 1972

Order No.:

Price: WF

Acc. No. NOAA

39152

DEPARTMENT OF COMMERCE

NOAA TECHNICAL MEMORANDUMS

National Environmental Satellite Service Series

The National Environmental Satellite Service (NESS) is responsible for the establishment and operation of the environmental satellite systems of NOAA.

NOAA Technical Memorandums facilitate rapid distribution of material that may be preliminary in nature and so may be published formally elsewhere at a later date. Publications 1 through 20 and 22 through 25 are in the earlier ESSA National Environmental Satellite Center Technical Memorandum (NESCTM) series (listed in NESS 30). The current NOAA Technical Memorandum NESS series includes 21, 26, and subsequent issuances.

Publications listed below are available from the National Technical Information Service, U.S. Department of Commerce, Sills Bldg., 5285 Port Royal Road, Springfield, Va. 22151. Prices on request. Order by accession number (given in parentheses). Information on memorandums not listed below can be obtained from Environmental Data Service (D831), 3300 Whitehaven St., NW, Washington, D.C. 20235.

NOAA Technical Memorandums

- NESS 21 Geostationary Satellite Position and Attitude Determination Using Picture Landmarks. William J. Dambeck, August 1972, 20 pp. (COM-72-10916)
- NESS 26 Potential of Satellite Microwave Sensing for Hydrology and Oceanography Measurements. John C. Alishouse, Donald R. Baker, E. Paul McClain, and Harold W. Yates, March 1971, 16 pp. (COM-71-00544)
- NESS 27 A Review of Passive Microwave Remote Sensing. James J. Whalen, March 1971, 8 pp. (COM-72-10546)
- NESS 28 Calculation of Clear-Column Radiances Using Airborne Infrared Temperature Profile Radiometer Measurements Over Partly Cloudy Areas. William L. Smith, March 1971, 12 pp. (COM-71-00556)
- NESS 29 The Operational Processing of Solar Proton Monitor and Flat Plate Radiometer Data. Henry L. Phillips and Louis R. ...
- NESS 30 Lim
Sat
- NESS 31 Pub
(CO
- NESS 32 On
fil
- NESS 33 Use
197
- NESS 34 Chr
Mar
- NESS 35 Mod
197
- NESS 36 A T
Pic
- NESS 37 Som
Ric
- NESS 38 Pub
111
- NESS 39 Ope
cha
- NESS 40 Con
1972

NOAA Technical Memorandum NESS 63

SNOW DEPTH AND SNOW EXTENT
USING VHRR DATA FROM THE NOAA-2 SATELLITE

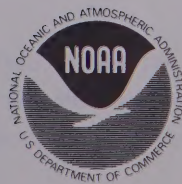
David F. McGinnis, Jr.
John A. Pritchard
Donald R. Wiesnet

Washington, D.C.
February 1975

UNITED STATES
DEPARTMENT OF COMMERCE
Frederick B. Dent, Secretary

NATIONAL OCEANIC AND
ATMOSPHERIC ADMINISTRATION
Robert M. White, Administrator

National Environmental
Satellite Service
David S. Johnson, Director



Rec'd: Mar 27/80
Order No.:
Price: WF
Acc. No: NOAA.

39152

CONTENTS

Abstract.....	1
I. Introduction.....	1
II. Southeast snow storm of February 9-10, 1973.....	1
III. NOAA-2 Satellite.....	2
IV. Imagery analysis.....	3
V. Digital tape analysis.....	5
VI. Results.....	9
VII. Conclusions.....	10
Acknowledgments.....	10
References.....	10

Mention of a commercial company or product does not constitute an endorsement by the NOAA National Environmental Satellite Service. Use for publicity or advertising purposes of information from this publication concerning proprietary products or the tests of such products is not authorized.

SNOW DEPTH AND SNOW EXTENT USING VHRR DATA FROM THE NOAA-2 SATELLITE

David F. McGinnis, Jr., John A. Pritchard, and Donald R. Wiesnet
National Environmental Satellite Service, NOAA, Washington, D.C.

ABSTRACT. The NOAA-2 environmental satellite provides daily coverage of the Earth in the visible (0.6-0.7 μm) and thermal (10.5-12.5 μm) spectral bands. The ground resolution of the Very High Resolution Radiometer (VHRR) is 1 km at nadir. This improved resolution in the visible permits more detailed observations of snow features than was possible with previous operational satellites. A densitometer examination of a visible-band image from Feb. 11, 1973, which shows heavy snow cover in considerable detail over areas extending from Alabama to North Carolina, indicates that, in general, there is direct correlation between increasing brightness and increasing snow depths. Digitized reflectance data from the study area were compared with prestorm bare-ground digitized reflectance data of Feb. 6, 1973, to determine the relation of snow reflectivity to snow depths. A parabolic regression analysis of greatest satellite brightness versus greatest snow depth for 211 data pairs produced a correlation coefficient of 0.84.

I. INTRODUCTION

The brightness of snow received as reflected radiation by visible-band sensors aboard meteorological satellites has been mentioned as a possible indicator of snow depth (Barnes and Bowley 1968, McClain 1973). Because of the much improved resolution of the Very High Resolution Radiometer (VHRR) data from the NOAA-2 environmental satellite, compared with the data available to previous investigators, a decision was made to test this hypothesis. Opportunity for such a study occurred on Feb. 11, 1973, immediately following a heavy snow storm that struck the southeastern part of the United States.

II. SOUTHEAST SNOW STORM OF FEBRUARY 9-10, 1973

The winter of 1973 will be remembered well in the southeastern United States for the storm of February 9 and 10. This storm, the result of the interaction of two sharply contrasting air masses, produced record snow depths. An outbreak of very cold Arctic air entered the

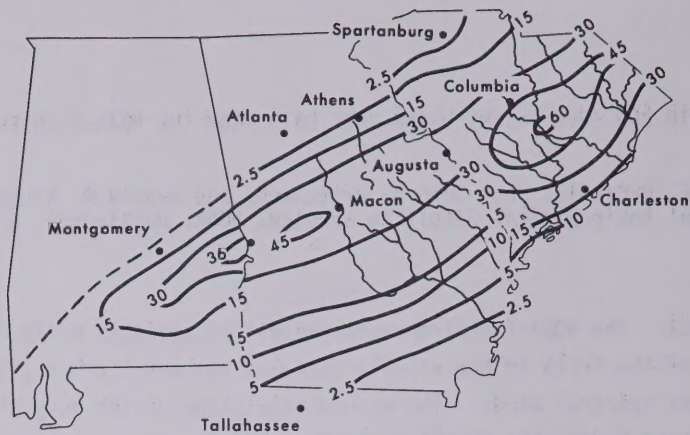


Figure 1.--Total snowfall, snow storm of Feb. 1-10, 1973

Northern Plains on Monday, Feb. 5, 1973. This large air mass plunged rapidly southward into Texas but made only slow progress eastward. By 1800 GMT (1300 LT) on Thursday, February 9, the leading edge of the cold air mass lay along the eastern slope of the Appalachian Mountains. Rain began falling in a broad band 350 km wide in the area of frontal convergence. Temperatures remained mild along the Atlantic seaboard until a developing cyclone drew in the very cold air just west of the Appalachians. The precipitation in Alabama and Georgia subsequently changed to freezing rain and sleet and then to snow during the morning and early afternoon of Friday, February 9. This snow spread into North Carolina and South Carolina as the deepening cyclonic disturbance moved northeastward into the Atlantic Ocean. Snow continued falling during most of Saturday in Georgia and the Carolinas, ending along most Carolina coastal sections after midnight. On Sunday morning, record snow depths were found on the ground at many locations in Alabama, Georgia, and the Carolinas. Figure 1 shows the total snowfall in Alabama, Georgia, and South Carolina as analyzed by the individual State climatologists from scattered point observations taken largely by untrained cooperative observers. Data and isopleths, originally in inches, were obtained from individual State climatological summaries for February 1973 (Environmental Data Service 1973). Despite inconsistent values from State to State, particularly along the Georgia-South Carolina border (where the 2.5-cm isopleth in northeastern Georgia matches the 15-cm isopleth in northwestern South Carolina), values in excess of 30 cm were reported throughout an extensive band from east-central Alabama through northeastern South Carolina. The dashed line represents the authors' interpretation of the 2.5-cm isopleth in Alabama. Storm totals, because of the warm ground and settling of the snow, were somewhat greater than observations taken Sunday morning at 1200 GMT after the storm's ending. Rapid clearing followed the storm; and at approximately 1545 GMT (1045 LT) on orbit 1489, Feb. 11, 1973, the NOAA-2 satellite viewed the cloud-free but snow-covered landscape (fig. 2).

III. NOAA-2 SATELLITE

The NOAA-2 satellite scans Earth in 25 orbits every 2 days at an altitude of approximately 1500 km in a sun synchronous near-polar orbit.¹ Essentially the same area of Earth is viewed

¹As of Dec. 17, 1974, NOAA 3 (with sensors identical to those on NOAA 2) was in a standby mode. NOAA 4 launched on Nov. 15, 1974, became the operational satellite on Dec. 17, 1974.



Figure 2.--Portion of the NOAA-2 VHRR visible (0.5-0.6 μm) image taken at 1545 GMT on Sunday, Feb. 11, 1973

every other day, although the orbit of the satellite progresses eastward about 1° of longitude every 25 orbits. Aboard the spacecraft are various sensors (Schwalb 1972), each with its own identical backup system.

Most important of the sensors for hydrological use is the VHRR. This instrument scans Earth in both the visible (0.6-0.7 μm) regions of the spectrum. The VHRR system generates analog signals that, after transmission to the readout station, are transformed into a photographic format. VHRR data are also available on digital tapes. With a resolution of approximately 1 km at nadir, the VHRR imagery is 4 times better in the visible and 10 times better in the thermal regions than data taken by instruments aboard NOAA 1 and earlier satellites.

One of the drawbacks of VHRR images is that panoramic distortion increases with increasing distance from the center line of the image. The image is built up through a combination of the satellite's forward motion in orbit and its VHRR scanning perpendicular to this motion. This distortion is caused, in part, by the curvature of Earth's surface and produces foreshortening of the image toward the horizon.

IV. IMAGERY ANALYSIS

Figure 2 shows the snow-covered area as seen in the visible range by the VHRR. State boundaries have been added to point out the distortion in the image and to provide reference points for location. These boundaries were added to figure 2 by using a Zoom Transfer Scope (ZTS), an optical device used to transfer information from unrectified satellite images to base maps, and vice versa. The distortion is greatest in the eastern portion of the image. A distinct western limit of the snow is evident, as well as a highly reflective (bright) strip in the center of the snow area, corresponding generally to the deepest snows shown in figure 1. Some land features in the snow belt, such as the swampy or heavily forested areas adjacent to many rivers, contrast sharply with adjacent areas in the snow-whitened land. The more heavily forested Piedmont Plateau in the western section of the snow area is mottled in appearance and is less bright than elsewhere. The 1-km resolution of the VHRR permits easy identification of many small rivers and also enables the analyst to determine the location of the western snow edge to within 8 km when drainage features are used as local reference points.

In figure 3 is a comparison of the snow extent viewed by the satellite with the 2.5-cm isopleth determined from ground observations on Sunday, February 11. Location of the zero isopleth, although the most useful for comparison with the satellite image, requires interpre-

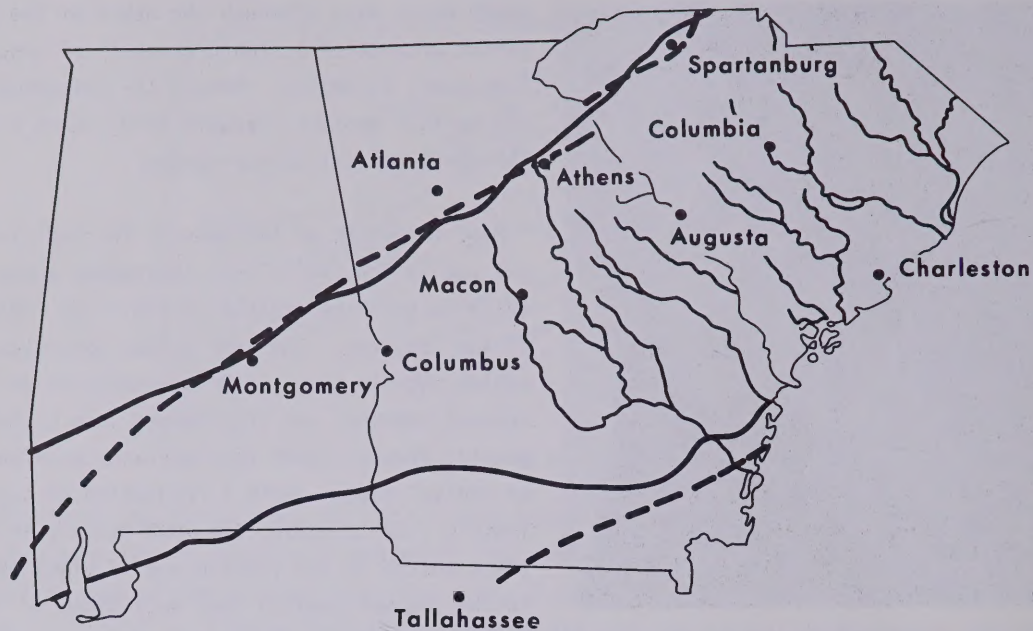


Figure 3.--Comparison of snow extent as viewed by the NOAA-2 satellite with the 2.5-cm isopleth determined from ground observations. The heavy solid line is the snow boundary based on the NOAA-2 VHR visible imagery; and the dashed line is the snow boundary based on ground observations.

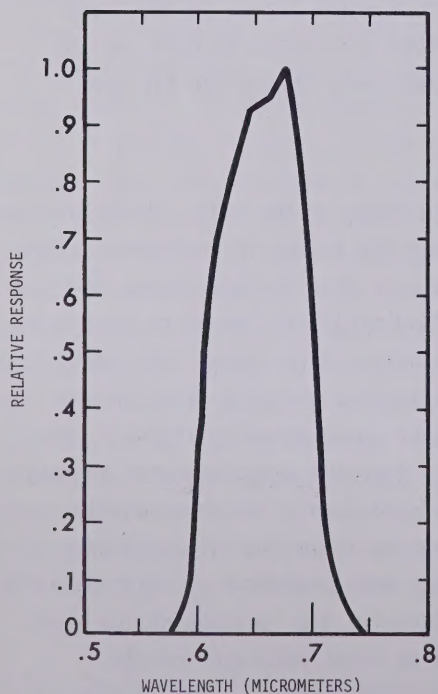


Figure 4.--NOAA-2 VHR visible relative spectral response curve (prelaunch)

tation of available ground truth. In areas where ground observations are few, accurate positioning of the zero isopleth is rather difficult. Fortunately, the sharp gradient in snow depths along the western boundary would place the edge of the snow only slightly north-west of the 2.5-cm isopleth. Note that Atlanta had no measurable snow during the storm although it lies less than 15 km from the 2.5-cm isopleth. Close agreement exists between ground and satellite observations along the western snow boundary. Even southeastern Georgia, where the edge of the snow line appears quite vague, a result of mixed precipitation and rather warm ground, satellite and ground maps of the snow extent coincide closely.

Analysis of the recorded brightnesses takes into account the system's limitations. Each pixel (picture element) of the VHR image covers an area of approximately 1 km² (at nadir) on the ground. The brightness value of each pixel thus represents an average response that may include dark, forested regions as well as high-

ly reflective open fields, even when both are snow covered. Also, the VHRR visible-band sensor is not a perfect detector. Figure 4 shows that the relative response of the detector falls short of perfect (1.0) throughout the design range of 0.6 to 0.7 μm and also senses some energy outside these limits.

The enhancement of land features by the differing reflectance of snow cover has been described. While this factor is useful for identifying and locating specific landmarks, it tends to mask the relation of snow brightness to snow depth. The aging of a snow pack is manifested in a reduction of the surface brightness--another factor to consider when attempting to relate snow brightness to snow depth. In our study of this relationship, the image was enhanced using a color densitometer. Various color schemes were tried, but none could discriminate more than three ranges of depth; these were 0 to 8 cm, 8 to 30 cm, and more than 30 cm. This breakdown into three ranges of depth is entirely qualitative and shows little improvement over the earlier estimates by Barnes and Bowley (1968) using lower resolution satellite imagery. One should note, however, that their study was confined to the Great Plains where variation in land use is much less of a problem. They were able to distinguish only three distinct levels of brightness within snow-covered areas; these correspond to depths of a trace to 2.5 cm, 2.5 to 10 cm, and greater than 10 cm.

In figure 5, a north-south densitometric trace through the snow area is shown on the left; the white strip through the image is the cross section that the trace represents. The densitometer trace is a quantitative measure of changes in photographic gray scales; it was produced from a black and white photograph using a color densitometer. Brightness values are represented along the horizontal axis, with increasing values to the left. Outside the snow area, brightness values are uniformly low. Within the snow-covered area, values are higher but show several fluctuations, which are a function of varying land use. The abrupt termination of the snow along the northwest boundary of the snow area is associated with a rapid decrease in brightness. The southern boundary of the snow area is more diffuse; thus, the decrease in brightness is gradual.

V. DIGITAL TAPE ANALYSIS

Digital computer printouts analogous to the pictorial display were produced from the VHRR analog tapes. The analog tapes were converted into nine-track digital tapes containing every scan line generated by the VHRR. Each scan line consists of individual, partially overlapping samples, two of which cover a 1-km^2 field of view. These elemental pieces of information can be averaged or combined in various schemes to meet the needs of the investigator.

In digital printout, 36 different alphanumeric characters are available to cover the 255 possible steps in the gray scale of the VHRR image. Usually, fewer than 255 steps are required for analysis. In the case of the February 11 image, only 63 gray levels were used

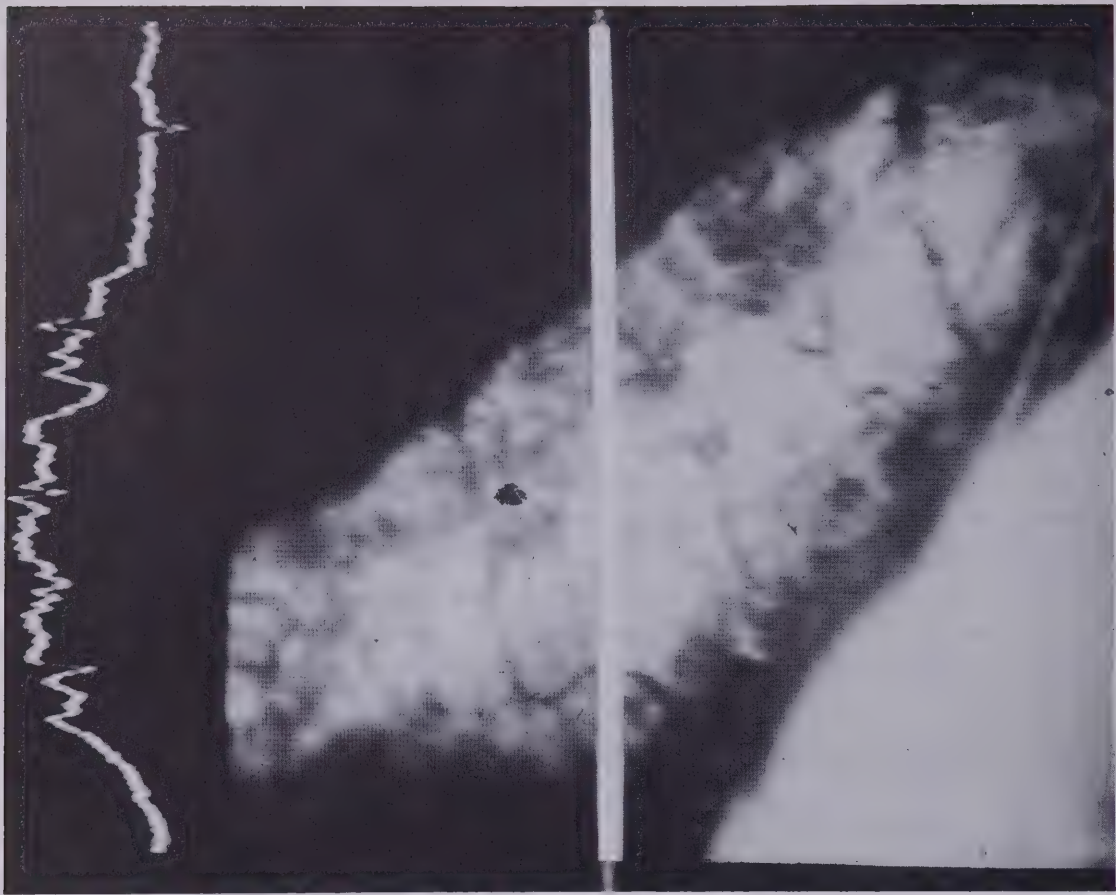


Figure 5.--Densitometric trace through portion of snow-covered area in South Carolina and Georgia

within the snow area to represent brightness variations ranging from dark swamps to bright snow-covered cleared fields. For this study, a three line four-sample (approximately 3 km) moving average was selected.

In pursuit of a snow depth-brightness relationship, seven brightness cross-sections of South Carolina, Georgia, and Alabama were plotted; each cross section was three scan lines (approximately 3 km) wide. A snow-free VHRR image (Feb. 5, 1973, orbit 1414) of this same area then was digitized to determine the brightness of the background with no snow. Then, the seven cross-sections from the snow-free data carefully were matched manually with those from the February 11 snow-depth data.

The eastward precession of the NOAA-2 satellite orbit, about 1° longitude every 2 days, prevented an exact matching of the two orbits. Using landmarks as reference points, however, we achieved a close correspondence. Figure 6 shows one of the seven matched pairs of cross sections. Note that the snow-free terrain is nearly the same brightness everywhere. The

zero values indicate the location of one of the two subsynchronization lines that are part of the VHRR data stream. The same swath under a blanket of snow varies widely in brightness, demonstrating how surface features are brought out by the snow. Subtraction of the snow-free terrain brightness from the snow brightness did not provide improved insight into the snow brightness-snow depth relationship.

Owing to the scarcity of detailed snow-depth measurements on the morning of Feb. 11, 1973, comparison of the snow brightness with ground truth necessitated substitution of snowfall totals [as provided in Environmental Data Service (1973)] for snow depth values. Arbitrary values between 1 and 256, corresponding to the 256 brightness increments detectable by the VHRR, were assigned to the 3-km data points in the seven cross-sections. A simple linear regression relating these brightness values to snowfall totals (assumed to vary linearly between the isopleths) was run for each cross section in another attempt to determine how well brightness relates to snow depth. The correlation coefficients ranged from 0.10 to 0.20, disappointingly low. These values probably were due to the use of 3-km averaged data, in which varying types of land use, some brighter than others, are combined to produce an averaged brightness value. Varying land use, when enhanced by snow, provides land marks for location but masks the snow-brightness to snow-depth relationship.

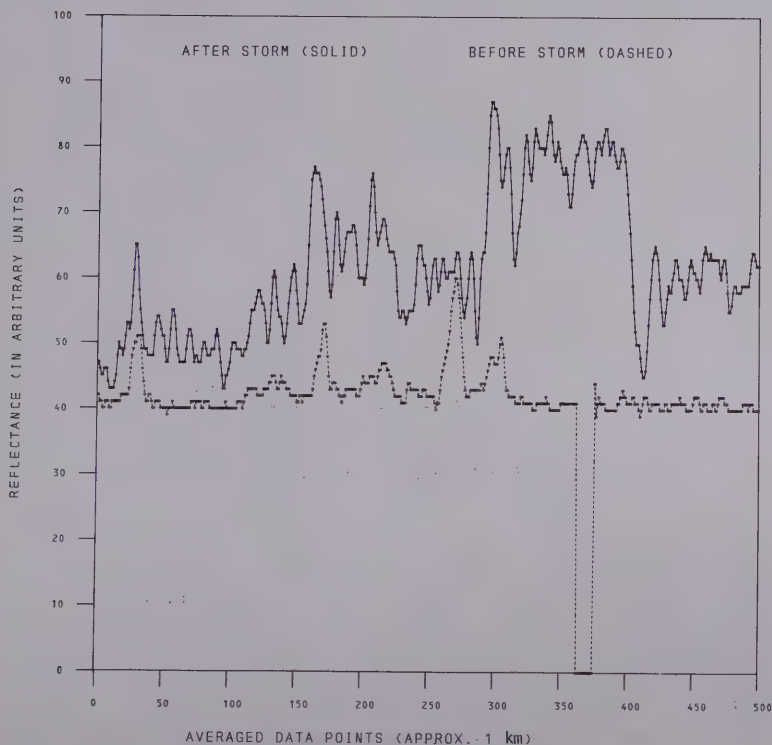


Figure 6.--Visible reflectance values before and after the snow storm for a 3-km cross section in Georgia and Alabama

A computer program was adapted to accept VHRR digital data and produce, at 1-km or 4-km resolution, histograms of brightness values at preset class intervals and provide the smallest and greatest brightness values for each 32 x 32 element area. The program also contours each area using the preset class intervals, thus providing an isopleth map. The 1,024 brightness values and annotations for location are included in the program.

Using the 1-km resolution option (32 x 32 km squares), we fitted a grid of 201 VHRR squares to figure 1. The greatest snow depth for each square (from fig. 1) was matched with the greatest brightness value. Linear and parabolic best fits were calculated for the data pairs with brightness as the dependent variable. Figure 7 shows the 201 data points and the best fitting linear and parabolic curves. Correlation coefficients were 0.80 for the straight line and 0.84 for the parabolic curve.

The parabolic fit of the data appears more consistent with the apparent relationship of brightness to snow depth. Rather small increases in depth when the snow is only several centimeters deep produce large increases in brightness. In this case, the snow covers more and more objects on the ground as it deepens, first individual blades of dormant grass, then small shrubs, then larger objects. Once the snow accumulates to about 25 cm, most small plants are covered, only the larger shrubs and plants (corn stalks to trees) remain visible and in most cases will remain uncovered except in some mountainous areas where extremely heavy snows occur.

Some radiation penetrating into a snow pack, if not absorbed by underlying vegetation and soil, eventually returns to the surface and contributes to the albedo. Giddings and LaChapelle (1961) demonstrated that absorption from an underlying black surface greatly reduced the al-

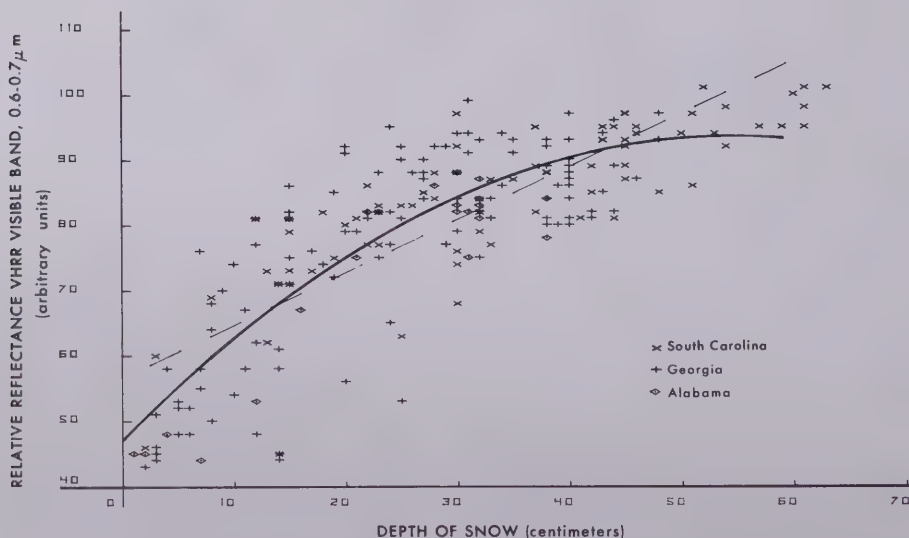


Figure 7.--Relation of relative VHRR visible reflectance to depth of snow

bedo of aged snow until snow depths exceeded 20 cm. Thus small increases in satellite-observed brightness may be observed even when tops of vegetation are being covered with 10 to 20 cm of snow.

Regarding data discontinuities in the snow isopleths at State boundaries, we used the following procedure. When a 32-km square fell across a State boundary, the greatest depth was determined using data from the State having the greater portion of the square. Also, some error in snow-depth estimates could occur because of the misalignment or distortion of the squares fitted to figure 1. Further, most of the snow-covered area in Alabama received some sunshine late in the day on Saturday, 10 February 1973, which probably melted a small amount of snow. The amount of snow remaining at the time of the satellite observation on Sunday morning, therefore, is believed to be slightly less than that indicated in figure 1. The scarcity of ground observations precluded a re-evaluation of snow depths. The effect of the Sun on the reflectivity of the snow and, thus, on the brightness recorded by the satellite also is not considered. Both of these effects caused by the Sun, however, trend in the same direction (i.e., toward decreasing values).

The curves derived from the data are for the NOAA-2 VHRR visible-sensor 1. Equivalent curves may be different for either NOAA-3 or NOAA-4 visible sensors or the other NOAA-2 VHRR visible sensor. The general relationship likely would remain, but with perhaps differing brightness limits. For this case, the lower limit of brightness (bare ground) is between 40 and 43; the upper limit of snow brightness is 101.

VI. RESULTS

The improved resolution of the VHRR over previous sensors on operational satellites permits mapping of snow limits to better than a 10-km resolution, which is an improvement over the 20- to 40-km resolution reported with earlier satellites (McClain 1973). Although the radiance data received from the satellite are unrectified, the enhancement of identifiable land features by the snow permits the precise location of snow boundaries of mesoscale resolution. Color renditions of the black and white imagery by means of a color densitometer, although subjective, do permit coarse estimates of snow depths, but the improvement over estimates made from earlier, lower resolution satellite sensors is minor.

Linear regression analyses of cross sections relating snow brightness to storm totals produced negligible correlation coefficients. A major reason for the lack of correlation is the variable brightness of snow-covered land used for different purposes. For snow-free winter conditions, all types of land surfaces in the southeastern United States appear almost uniformly bright (lower curve in fig. 6). When enhanced by a deep snow cover, however, the varying land surfaces reflect very differently (upper curve in fig. 6). Under the same depth of snow, open farmland appears very bright, wet swampy areas adjacent to the major rivers are dark, and forested areas appear in differing intermediate tones depending upon density and type of trees.

A significant correlation of 0.84 was achieved, however, when the greatest brightness value in a given 32 x 32 km square was paired with the greatest snow depth for the same square. Using the greatest brightness within a particular region is, in effect, searching for the clearings and open areas that are free of trees and other nonsnow-covered objects that lower the average brightness of the 1-km element.

VII. CONCLUSIONS

For the case studied (i.e., freshly fallen snow over an area of widely varied land use), the VHRR provides a synoptic picture of snow extent not possible from point observations on the ground. The 1-km resolution of the VHRR sensors permits positioning of snow limits to within 10 km, some two to four times better than that possible with data from earlier operational satellites.

Snow-depth estimates correlate well with snow brightness. The parabolic relationship indicates that a rapid increase in brightness corresponds to increases in snow depths when depths are less than 25 cm; for depths exceeding 25 cm, much smaller brightness increases are encountered as depths increase.

ACKNOWLEDGMENTS

The authors wish to express appreciation to E. Paul McClain for initiating discussion with respect to the investigation of maximum brightness versus snow depth. Michael C. McMillan and Marilyn Varnadore are also gratefully acknowledged for computations to determine correlation coefficients and for computer programming resulting in figure 6, respectfully.

REFERENCES

- Barnes, J.C., and Bowley, C.J., Operational Guide for Mapping Snow Cover From Satellite Photography, Allied Research Associates, Inc., Concord, Mass., 1968, 116 pp.
- Environmental Data Service, Climatological Data Alabama, Climatological Data Georgia, and Climatological Data South Carolina, Vol. 79, No. 2, National Climatic Center, National Oceanic and Atmospheric Administration, U.S. Department of Commerce, Asheville, N.C., Feb. 1973.
- Giddings, J.C., and LaChapelle, E., "Diffusion Theory Applied to Radiant Energy Distribution and Albedo of Snow," Journal of Geophysical Research, Vol. 66, No. 1, Jan. 1961, pp. 181-189.
- McClain, E. Paul, "Snow Survey From Earth Satellites--a Technical Review of Methods," WMO/IHD Report No. 19, WMO No. 353, World Meteorological Organization/International Hydrological Decade, Geneva, Switzerland, 1973, 42 pp.
- Schwalb, A. "Modified Version of the Improved TIROS Operational Satellite (ITOS D-G)," NOAA Technical Memorandum NESS 35, National Environmental Satellite Service, National Oceanic and Atmospheric Administration, U.S. Department of Commerce, Washington, D.C., Apr. 1972, 48 pp.

- NESS 41 Effect of Orbital Inclination and Spin Axis Attitude on Wind Estimates From Photographs by Geosynchronous Satellites. Linwood F. Whitney, Jr., September 1972, 32 pp. (COM-72-11499)
- NESS 42 Evaluation of a Technique for the Analysis and Forecasting of Tropical Cyclone Intensities From Satellite Pictures. Carl O. Erickson, September 1972, 28 pp. (COM-72-11472)
- NESS 43 Cloud Motions in Baroclinic Zones. Linwood F. Whitney, Jr., October 1972, 6 pp. (COM-73-10029)
- NESS 44 Estimation of Average Daily Rainfall From Satellite Cloud Photographs. Walton A. Follansbee, January 1973, 39 pp. (COM-73-10539)
- NESS 45 A Technique for the Analysis and Forecasting of Tropical Cyclone Intensities From Satellite Pictures (Revision of NESS 36). Vernon F. Dvorak, February 1973, 19 pp. (COM-73-10675)
- NESS 46 Publications and Final Reports on Contracts and Grants, 1972. NESS, April 1973, 10 pp. (COM-73-11035)
- NESS 47 Stratospheric Photochemistry of Ozone and SST Pollution: An Introduction and Survey of Selected Developments Since 1965. Martin S. Longmire, March 1973, 29 pp. (COM-73-10786)
- NESS 48 Review of Satellite Measurements of Albedo and Outgoing Long-Wave Radiation. Arnold Gruber, July 1973, 12 pp. (COM-73-11443)
- NESS 49 Operational Processing of Solar Proton Monitor Data. Louis Rubin, Henry L. Phillips, and Stanley R. Brown, August 1973, 17 pp. (COM-73-11647/AS)
- NESS 50 An Examination of Tropical Cloud Clusters Using Simultaneously Observed Brightness and High Resolution Infrared Data From Satellites. Arnold Gruber, September 1973, 22 pp. (COM-73-11941/4AS)
- NESS 51 SKYLAB Earth Resources Experiment Package Experiments in Oceanography and Marine Science. A. L. Grabham and John W. Sherman, III, September 1973, 72 pp. (COM 74-11740/AS)
- NESS 52 Operational Products From ITOS Scanning Radiometer Data. Edward F. Conlan, October 1973, 57 pp. (COM-74-10040)
- NESS 53 Catalog of Operational Satellite Products. Eugene R. Hoppe and Abraham L. Ruiz (Editors), March 1974, 91 pp. (COM-74-11339/AS)
- NESS 54 A Method of Converting the SMS/GOES WEFAX Frequency (1691 MHz) to the Existing APT/WEFAX Frequency (137 MHz). John J. Nagle, April 1974, 18 pp. (COM-74-11294/AS)
- NESS 55 Publications and Final Reports on Contracts and Grants, 1973. NESS, April 1974, 8 pp. (COM-74-11108/AS)
- NESS 56 What Are You Looking at When You Say This Area Is a Suspect Area for Severe Weather? Arthur H. Smith, Jr., February 1974, 15 pp. (COM-74-11333/AS)
- NESS 57 Nimbus-5 Sounder Data Processing System, Part I: Measurement Characteristics and Data Reduction Procedures. W.L. Smith, H. M. Woolf, P. G. Abel, C. M. Hayden, M. Chalfant, and N. Grody, June 1974, 99 pp. (COM-74-11436/AS)
- NESS 58 The Role of Satellites in Snow and Ice Measurements. Donald R. Wiesnet, August 1974, 12 pp. (COM-74-11747/AS)
- NESS 59 Use of Geostationary-Satellite Cloud Vectors to Estimate Tropical Cyclone Intensity. Carl O. Erickson, September 1974, 37 pp. (COM-74-11762/AS)
- NESS 60 The Operation of the NOAA Polar Satellite System. Joseph J. Fortuna and Larry N. Hambrick, November 1974, 127 pp.
- NESS 61 Potential Value of Earth Satellite Measurements to Oceanographic Research in the Southern Ocean. E. Paul McClain, January 1975, 18 pp.
- NESS 62 A Comparison of Infrared Imagery and Video Pictures in the Estimation of Daily Rainfall From Satellite Data. Walton A. Follansbee and Vincent J. Oliver, January 1975, 14 pp.



0 1620 0332 4165